Supporting Information

Schmelz et al. 10.1073/pnas.1014714108

SI Text

Characterization of Maize Diterpenoids. GC/MS analysis of kauralexins A3, B2, and B3 suggested a kaurane skeleton. Tables S1–S3 show the ^{1}H correlation, ^{13}C correlation, heteronuclear multiple-bond correlation (HMBC), and NOESY correlation for kauralexins A3, B2, and B3, respectively. Comparisons with proton and carbon assignments of known kauranes and NOESY data for kauralexins A3, B2, and B3 suggested that the functional (COOH or CHO) group at C19 is axially substituted to the C4 carbon, the methyl group (C20) at C10 has an axial substitution, and protons of C14 (the bridge protons) were on the same side as the C20 methyl groups (1–6). The protons on C5 and C9 were found to be opposite those of the C20 methyl group, previously implicated as the β-position (7). We have indicated the relative stereochemistry for kauralexins A3, B2, and B3 on an "*ent*-kaurane" structure, based on prior literature of such natural substances from plants (1, 2, 5, 7–9).

Kauralexin A3. The ^{1}H and ^{13}C NMR data are presented in Table S1. The aldehyde proton signal at δ 9.73 suggested an axial substitution to C4, where the proton signal of aldehyde for axial position was reported to be δ 9.73 (τ 0.27) and the equatorial position was found at δ 9.24 (4, 10). Additionally, the aldehyde proton signal showed a doublet, which is in agreement with the findings of Henrick and Jefferies (4), wherein axial aldehyde protons to C4 showed a doublet with J = 1.2 Hz and all equatorial aldehyde protons showed a singlet. This was further supported by ^{13}C chemical shifts of C4 and C5. The chemical shifts of C4 (δ 48.7) and C5 (δ 56.8) are consistent with reported chemical shifts of C4 (δ 48.5, 48.3) and C5 (δ 56.7, 56.2) (3, 8). Also, proton signals of methyl groups at δ 0.99 for C4-CH_3 and δ 0.85 for C10-CH_3 are in agreement with the results of Henrick and Jeffries (4), wherein C4-CH_3 protons showed a signal at δ 0.99 (τ 9.01) and C10-CH_3 protons showed a signal at δ 0.86 (τ 9.14) when CHO was axially substituted on C4.

Kauralexin B2. The ^{1}H and ^{13}C NMR data of kauralexin B2 are shown in Table S2. An axial position of COOH at C4 was suggested by hindered methylation of acid or saponification of methyl ester (4). Axial substitution of COOH to C4 was further supported by ^{13}C NMR chemical shifts of C4 (δ 43.5) and C5 (δ 56.29), wherein axial COOH substitution was reported to be δ 43.7, δ 43.8, and δ 44.1 for C4 and δ 56.0–58.4 for C5 (6, 9–12) and equatorial COOH substitution was reported to be δ 47.6–47.9 for C4 and δ 57.1–57.3 for C5 (6, 9, 10). Additional support comes from proton signals of methyl groups on C4 and C10 for an axially located COOH group on C4. The proton signal for C4-CH_3 (C18) δ 1.24 and C10-CH_3 (C20) δ 0.99 is in agreement with studies in which C4-CH_3 signal is reported to be δ 1.23–1.24, 1.26 and C10-CH_3 is reported δ 0.93–0.94, 1.00 when the COOH group is axially substituted to C4 (4, 11).

Kauralexin B3. Kauralexin B3 ^{1}H and ^{13}C NMR data are presented in Table S3. Similar to kauralexin A3, the aldehyde proton signal at δ 9.74 with a doublet (J = 1.2 Hz) suggested an axial substitution to C4 consistent with the findings of Henrick and Jeffries (4). An axial position of the aldehyde was further supported by ^{13}C chemical shifts of C4 and C5. The chemical shifts of C4 (δ 48.57) and C5 (δ 56.33) are consistent with kauralexin A3 (Table S1) and the reported chemical shifts for C4 and C5 (3, 8). Additionally, proton signal of the methyl group (C18) of C4-CH_3 at δ 1.01 is in agreement with that of kauralexin A3 (Table S1) and similar kaurane structures, wherein C4-CH_3 protons showed a signal at δ 0.99 (τ 9.01) and δ 1.00 when CHO was axially substituted on C4 (3, 4).

NMR Analysis of Kauralexins A3, B2, and B3. Kauralexins (~0.5 mg) were dried under an N_2 stream, resuspended in 150 μL of $CDCl_3$ (Cambridge Isotope Laboratories, Inc.), and placed in 2.5-mm NMR tubes (Norell). 2D NMR spectroscopy, including double-quantum filtered correlation spectroscopy, heteronuclear single-quantum coherence, HMBC, and NOESY, was used for analyte characterization. All NMR spectra were acquired at 22 °C using a 5-mm TXI cryoprobe (Bruker Corporation) and a Bruker Avance II 600 console (600 MHz for ^{1}H and 151 MHz for ^{13}C). Residual $CHCl_3$ was used to reference chemical shifts to δ($CHCl_3$) = 7.26 ppm for ^{1}H and δ($CHCl_3$) = 77.36 ppm for ^{13}C (13). NMR spectra were processed using Bruker Topspin 2.0 and MestReNova (Mestrelab Research) software packages. Direct ^{13}C NMR data for kauralexin B3 were collected on a Bruker Avance 500 console (500 MHz for ^{1}H and 126 MHz for ^{13}C) with a 5-mm broadband probe at a sample temperature of 27 °C.

1. Bohlmann F, Suding H, Cuatrecasas J, King RM, Robinson H (1980) Naturally occurring terpene derivatives. Part 240. New diterpenes from the subtribe Espeletiinae. *Phytochemistry* 19:267–271.
2. Bohlmann F, Suding H, Cuatrecasas J, Robinson H, King RM (1980) Naturally occurring terpene derivatives. Part 286. Tricyclic sesquiterpenes and further diterpenes from *Espeletiopsis* species. *Phytochemistry* 19:2399–2403.
3. Gao F, Miski M, Gage DA, Norris JA, Mabry TJ (1985) Terpenoids from *Viguiera potosina*. *J Nat Prod* 48:489–490.
4. Henrick CA, Jefferies PR (1964) The chemistry of the Euphorbiaceae. VII. The diterpenes of *Ricinocarpos stylosus*. *Aust J Chem* 17:915–933.
5. Herz W, Kulanthaivel P, Watanabe K (1983) *Ent*-kauranes and other constituents of three *Helianthus* species. *Phytochemistry* 22:2021–2025.
6. Rahman A-U, Ahmad VU (1992) *13C-NMR of Natural Products* (Plenum, New York).
7. Vorbrueggen H, Djerassi C (1962) Alkaloid studies. XXXVI. Complete absolute configuration of the diterpene alkaloids of the Garrya and Atisine groups and their direct correlation with the phyllocladene-type diterpenes. *J Am Chem Soc* 84: 2990–2997.
8. Chen CY, Chang FR, Cho CP, Wu YC (2000) *ent*-kaurane diterpenoids from *Annona glabra*. *J Nat Prod* 63:1000–1003.
9. Monte FJQ, Dantas EMG, Braz FR (1988) New diterpenoids from *Croton argyrophylloides*. *Phytochemistry* 27:3209–3212.
10. Bohlmann F, Jakupovic J, King RM, Robinson H (1980) Naturally occurring terpene derivatives. Part 257. New *ent*-atisirenic- and *ent*-kaurenic acid-derivatives from *Helianthus* species. *Phytochemistry* 19:863–868.
11. Harrigan GG, Bolzani VDS, Gunatilaka AAL, Kingston DGI (1994) Kaurane and trachylobane diterpenes from *Xylopia aethiopica*. *Phytochemistry* 36:109–113.
12. Jakupovic J, et al. (1989) Diterpenes and other constituents from Australian *Helichrysum* and related species. *Phytochemistry* 28:543–551.
13. Gottlieb HE, Kotlyar V, Nudelman A (1997) NMR chemical shifts of common laboratory solvents as trace impurities. *J Org Chem* 62:7512–7515.

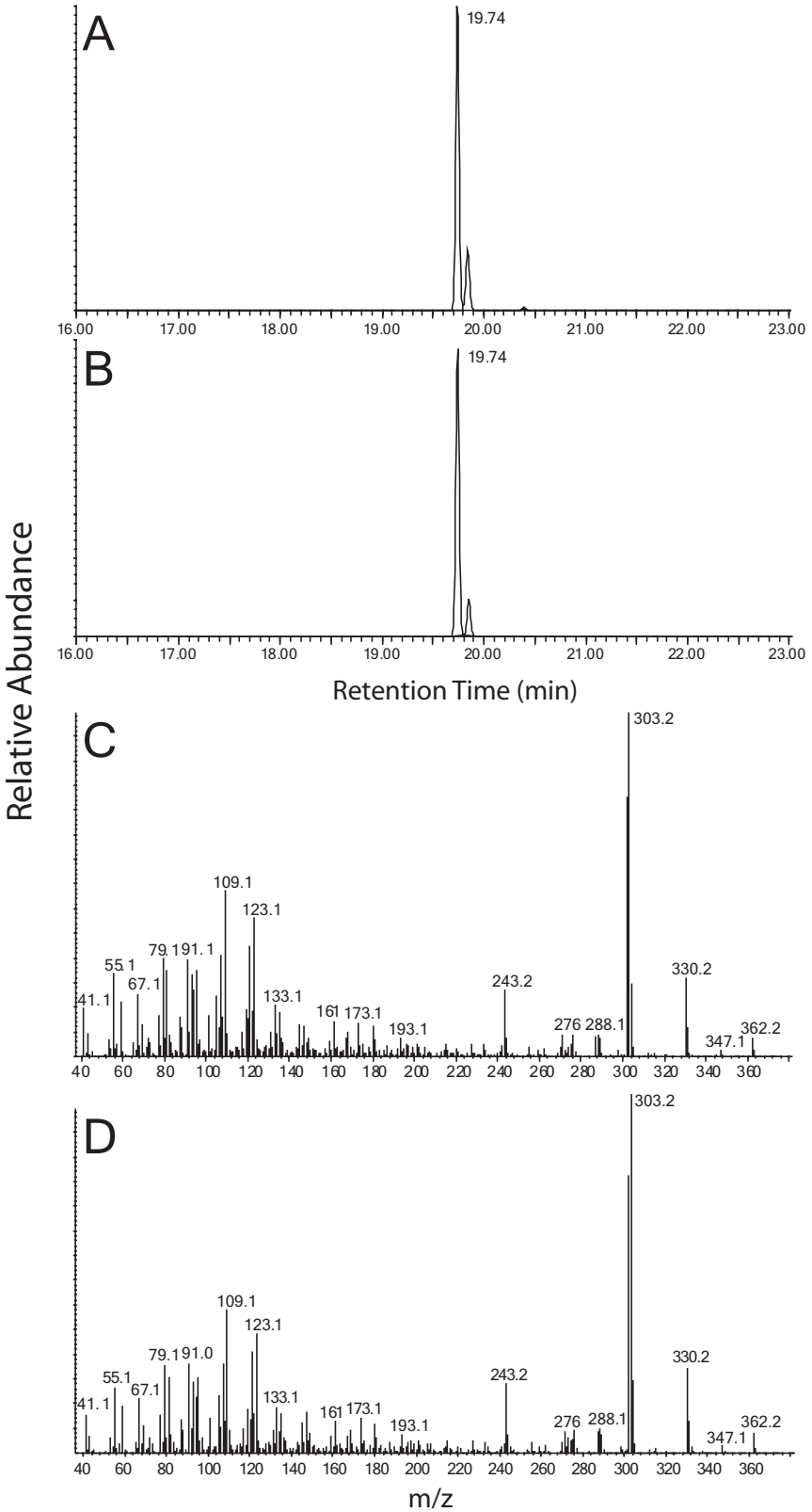

Fig. S1. Maize kauralexin A2 is consistent with *ent*-kauran-17,19-dioic acid present in the *Annona squamosa* roots. (*A*) GC/MS CI $[M + H]^+$ 363-selected ion trace and retention time (DB-35) of maize kauralexin A2. (*B*) Respective GC/MS trace of *ent*-kauran-17,19-dioic acid from *A. squamosa* (TARS-17880) roots. (*C*) EI spectra of maize kauralexin A2. (*D*) EI spectra of *ent*-kauran-17,19-dioic acid from *A. squamosa* roots. In these analyses, all carboxylic acid functional groups have been derivatized to their respective methyl esters.

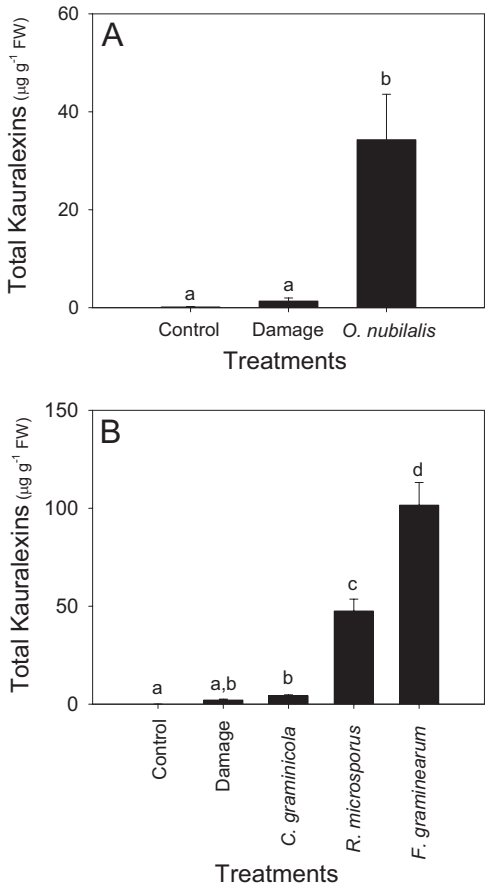

Fig. S2. Long-term *Ostrinia nubilalis* stem herbivory and fungal infection results in high levels of kauralexin accumulation. (*A*) Average (n = 3, ±SEM) total kauralexins in maize stems 8 d following no treatment (Control), mechanical damage (Damage), or *O. nubilalis* herbivory (*O. nubilalis*). (*B*) Average (n = 4, ± SEM) total kauralexins in maize stems 48 h following no treatment (Control) or mechanical damage plus either H_2O (Damage), *Colletotrichum graminicola* spores, *Rhizopus microsporus* spores or *Fusarium graminearum* spores. Each slit stem received 100 μL of pure H_2O or H_2O containing 1×10^7 spores·mL^{-1} of the respective fungi. Total kauralexins in the Control were 42.2 ± 13.8 ng·g^{-1} FW, and thus are not visible on this scale. Within plots, different letters (a–d) represent significant differences ($P < 0.007$ for all ANOVAs; $P < 0.05$ for Tukey test corrections for multiple comparisons).

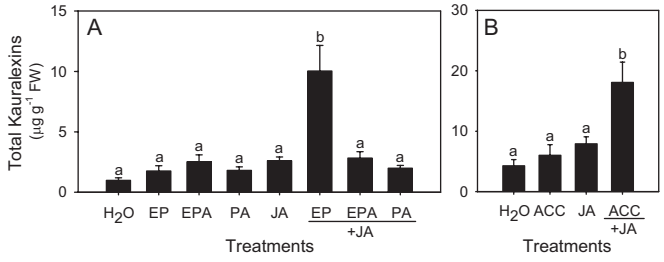

Fig. S3. Stem kauralexin accumulation is promoted by the interaction of JA and E. (*A*) Average (n = 4, ±SEM) total kauralexins in maize stems 24 h following mechanical damage plus H_2O; EP; ethylphosphonic acid (EPA); phosphonic acid (PA); JA; or a combination of JA + EP, JA + EPE, or JA + P. (*B*) Average (n = 4, ± SEM) total kauralexins in maize stems 24 h following mechanical damage plus H_2O, ACC, JA, or JA + ACC. JA was applied at 100 nmol·plant^{-1} as a Na^+ salt, and EP, EPA, PA, and ACC were applied at 33 nmol·plant^{-1}. Each chemical was transferred to the slit stem in 10 μL of H_2O. Within plots, different letters (a and b) represent significant differences ($P < 0.0015$ for all ANOVAs; $P < 0.05$ for Tukey test corrections for multiple comparisons).

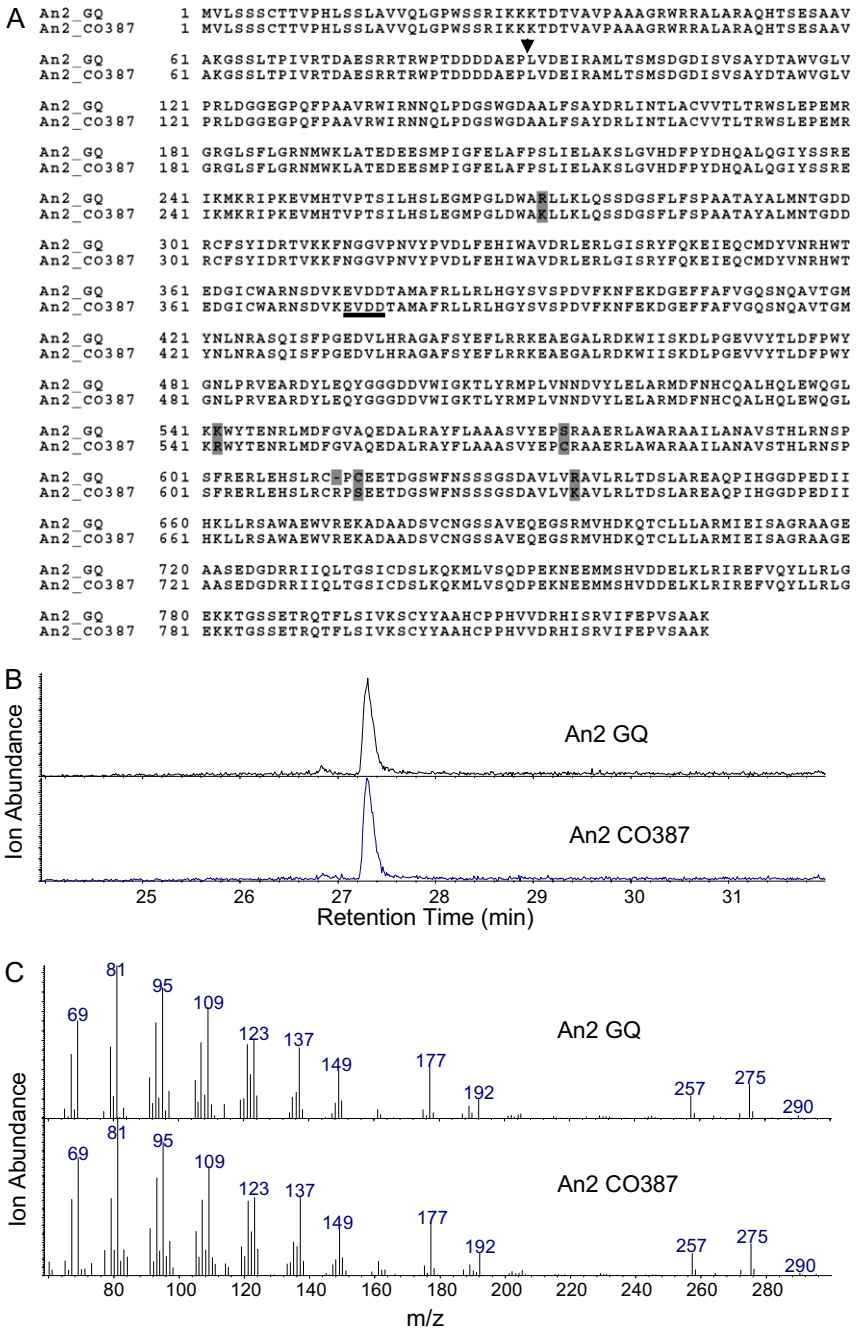

Fig. S4. Predicted translation of *Z. mays* var. Golden Queen *An2* reveals a high level of sequence conservation with the CO387 inbred line and maintains functional *ent*-CPS activity in bacterial expression assays. (*A*) Comparison of the predicted proteins encoded by *An2* from Golden Queen and CO387 (1). The five amino acid differences and single amino acid deletion are highlighted in gray. The conserved (D,E)XDD motif functionally associated with the catalytic activity of class II terpene synthases is underlined, and the site of truncation for recombinant expression is indicated by an arrowhead (2, 3). Total RNA was extracted by TRIzol RNA reagent (Invitrogen) from Golden Queen tissue, and overlapping cDNA clones were obtained by RT-PCR, which used random decamers, Moloney murine leukemia virus reverse transcriptase (MMLV RT) (Ambion), and Platinum Taq (Invitrogen) polymerase. PCR primers were based on the National Center for Biotechnology Information Reference Sequence NM_001111787.1 for CO387 and included the following: *An2* Forward 1, 5′-TGCGTTTCAGTGCGAGTAT-TATAGTA-3′; *An2* Reverse 1, 5′-GCAGCTTCGCCCAGTCTAGCC-3′; *An2* Forward 2, 5′-CTAGCCAAGAGTCTGGGCGTCC-3′; *An2* Reverse 2, 5′-CATCCTAGCCAGCT-CAAGATACAC-3′; *An2* Forward 3, 5′-GATTGAGCAGTGCATGGACT-3′; and *An2* Reverse 3, 5′-GAGTTTGGGACACAGCGATTG-3′. The amplicon sizes for the three primer sets were 957, 927, and 1,619 bp, respectively. The cDNAs were cloned into pCR2.1 T/A vector (Invitrogen), sequenced, and then aligned with MAFFT (http://www.ebi.ac.uk/Tools/mafft/). (*B*) GC/MS-selected ion trace (*m/z* = 275) of *ent*-copalol produced from bacterially expressed Golden Queen and CO387 AN2 in the presence of geranylgeranyl diphosphate (GGPP) and phosphatase confirms functional *ent*-CPS activity. A pseudomature version of the Golden Queen AN2 was recombinantly expressed in *Escherichia coli* following procedures previously described (1, 4). A truncation of *An2*, eliminating nucleotides encoding the first 90 amino acids, was amplified using the primers Forward, 5′-CACCCTGGTCGACGAGATC-3′, and Reverse, 5′-TTATTTTGCGGCGGAAACAGG-3′, and then cloned into pENTR/D-TOPO (Gateway system; Invitrogen). The clone was transferred via directional recombination to the pDEST15 (Gateway system) vector for expression as a GST fusion protein and transformed into BL21 CodonPlus (DE3) RIPL *E. coli* (Stratagene). Cultures grown to midlog phase at 37 °C were induced (1 mM isopropyl-β-D-thiogalactopyranoside) and shifted to 16 °C for overnight expression. Cells were harvested by centrifugation and lysed by sonication (30 s,

Legend continued on following page

continuous, output setting 5; Omni Ruture 250; Omni International Inc.), and crude lysate was passed through a buffer exchange/PD-5 desalting column (GE Healthcare) and eluted with assay buffer (50 mM Hepes, 100 mM KCl, 7.5 mM MgCl, 5% glycerol (vol/vol), and 5 mM DTT). Enzymatic analysis reactions using 4 mL of effluent lysate were initiated by the addition of 10 μM GGPP and carried out for 1 h at 30 °C before overnight dephosphorylation with calf intestinal phosphatase (New England Biolabs) and extraction by organic solvents (1:1 pentane/ethyl acetate). Extracts were concentrated under a gentle flow of N_2 and resuspended in 50 μL of ethyl acetate for GC/MS analysis. GC/MS was performed using a DB-35MS (30 m × 0.25 mm × 0.25 μm; Agilent) column on an Agilent 6890N GC instrument with a 5975B inert XL EI/CI mass selective detector. Helium was the carrier gas (flow rate of 0.7 mL·min^{-1}), a cool on-column injection of 1 μL was used, and a temperature gradient of 10 °C per min^{-1} from 30 °C (2.5-min hold) to 300 °C was applied. The construct containing *An2* from CO387 was kind gift obtained from Reuben Peters (Iowa State University, Ames, IA) and used as an *ent*-CPS positive control (1). (*C*) Full EI-GC/MS spectra of *ent*-copalol produced from bacterially expressed Golden Queen AN2 and the CO387 AN2-positive control.

1. Harris LJ, et al. (2005) The maize *An2* gene is induced by *Fusarium* attack and encodes an *ent*-copalyl diphosphate synthase. *Plant Mol Biol* 59:881–894.
2. Peters RJ, Croteau RB (2002) Abietadiene synthase catalysis: Conserved residues involved in protonation-initiated cyclization of geranylgeranyl diphosphate to (+)-copalyl diphosphate. *Biochemistry* 41:1836–1842.
3. Peters RJ, Ravn MM, Coates RM, Croteau RB (2001) Bifunctional abietadiene synthase: Free diffusive transfer of the (+)-copalyl diphosphate intermediate between two distinct active sites. *J Am Chem Soc* 123:8974–8978.
4. Xu M, Hillwig ML, Prisic S, Coates RM, Peters RJ (2004) Functional identification of rice *syn*-copalyl diphosphate synthase and its role in initiating biosynthesis of diterpenoid phytoalexin/allelopathic natural products. *Plant J* 39:309–318.

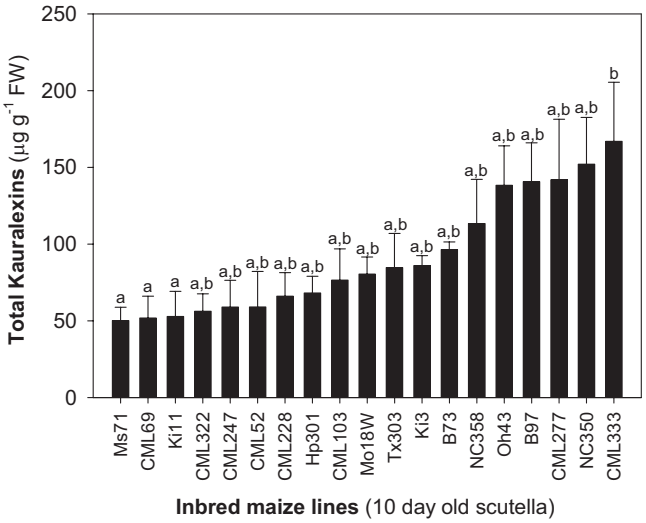

Fig. S5. Elevated kauralexin levels are ubiquitous in the scutella of maize seedlings and display significant variation between inbred lines. Total kauralexins (n = 4, ±SEM) in the scutella of 10-d-old maize seedlings from 19 diverse inbred maize lines, including Ms71, CML69, Ki11, CML322, CML247, CML52, CML288, Hp301, CML103, Mo18W, Tx303, Ki3, B73, NC358, Oh43, B97, CML277, NC350, and CML333. Different letters (a and b) represent significant differences (P < 0.001 for all ANOVAs; P < 0.05 for Tukey test corrections for multiple comparisons).

Table S1. Kauralexin A3 ^{1}H (600 MHz), ^{13}C (151 MHz), HMBC, and NOESY NMR spectroscopic data in $CDCl_3$

Table S1 (PDF)

Table S2. Kauralexin B2 ^{1}H (600 MHz), ^{13}C (151 MHz), HMBC, and NOESY NMR spectroscopic data in $CDCl_3$

Table S2 (PDF)

Table S3. Kauralexin B3 ^{1}H (600 MHz), ^{13}C (151 MHz), HMBC, and NOESY NMR spectroscopic data in $CDCl_3$

Table S3 (PDF)